Reduced order modeling of the Shell-Prenflo entrained flow gasifier

Citation: Gazzani, Matteo, Giampaolo Manzolini, Ennio Macchi, and Ahmed F. Ghoniem. "Reduced Order Modeling of the Shell–Prenflo Entrained Flow Gasifier." Fuel 104 (February 2013): 822-837.

As Published: http://dx.doi.org/10.1016/j.fuel.2012.06.117

Publisher: Elsevier

Persistent URL: http://hdl.handle.net/1721.1/105407

Version: Author's final manuscript: final author's manuscript post peer review, without publisher's formatting or copy editing

REDUCED ORDER MODELING OF THE SHELL-PRENFLO ENTRAINED FLOW GASIFIER

Matteo Gazzani[a*], Giampaolo Manzolini[a], Ennio Macchi[a], and Ahmed Ghoniem[b]

a) Politecnico di Milano, Dipartimento di Energia
Via Lambruschini 4 – 20156 Milano – Italy
www.gecos.polimi.it

b) Massachusetts Institute of Technology, Department of Mechanical Engineering
77 Massachusetts Avenue – Cambridge, MA US
web.mit.edu/rgd/www/

Abstract

Pre-combustion capture applied to an Integrated Gasification Combined Cycle is a promising solution for greenhouse gas emission's mitigation. For optimal design and operation of this cycle, detailed simulation of entrained flow gasifiers and their integration in the flowsheet analysis is required. This paper describes the development of a Reduced Order Model (ROM) for the Shell-Prenflo gasifier family, used for chemicals and power production because of its high efficiency and compatibility with a wide range of coal quality. Different from CFD analysis, ROM is computationally very efficient, taking around 1 min in a typical desktop or laptop computer, hence enabling the integration of the gasifier model and the overall power plant flowsheet simulation. Because of the gasifier complexity, which includes several gas recirculation loops and a membrane wall, particular attention is paid to: (i) the two-phase heat exchange process in the gasifier wall; and, (ii) the syngas quench process. Computed temperature, composition, velocity and reaction rate profiles inside the gasifier show good agreement with available data. The calculated Cold Gas Efficiency is 82.5%, close to the given value of 82.8%. Results and several sensitivity analyses describe the implementation of the model to explore the potential for operating gasifiers beyond the design point.

Keywords: Shell Gasifier; Prenflo Gasifier; IGCC; Entrained flow gasifier; CO_2 pre-combustion capture; Reduced order model

---

Nomenclature and Acronyms

ACM: Aspen Custom Modeler
ASU: Air Separation Unit
CFD: Computational Fluid Dynamic
CGE: Cold Gas Efficiency
COS: Carbonyl Sulfide
DSZ: Downstream Zone
ERZ: External Recirculation Zone
GT: Gas Turbine
HHV: Higher Heating Value
HP: High Pressure
HPHT: High Pressure High Temperature
IGCC: Integrated Gasification Combined Cycle
IP: Intermediate Pressure
IRZ: Internal Recirculation Zone
JEZ: Jet Expansion Zone
LH: Lock Hopper
LHV: Lower Heating Value
LP: Low Pressure
PFR: Plug Flow Reactor
ROM: Reduced Order Model
RNM: Reactor Network Model
WGS: Water Gas Shift
WSR: Well Stirred Reactor

[*] Corresponding author: tel +39 02 2399 3935
Email: matteo.gazzani@mail.polimi.it
www.gecos.polimi.it

Subscripts
Th: thermal
El: Electrical

1 Introduction

Rising world energy demand has mostly been met by expanding the use of fossil fuels, resulting in higher concentrations of carbon dioxide in the atmosphere. The possible consequences of these trends, in particular global warming, have driven the search for alternative electricity generation technologies capable of limiting CO_2 emissions. It is very likely that carbon dioxide reduction will have to be achieved while fossil fuels continue to be the major source of primary energy for several decades to come. CO_2 reduction must be pursued using a portfolio of different approaches. One of these, carbon dioxide capture and storage, is recognized as one of the most promising options because it addresses the impact of the largest primary energy sources and the largest source of CO_2. Among the three main routes for CO_2 capture in electric energy production, pre-combustion capture, which is compatible with efficient integrated gasification combined cycle power plants adds, in some estimates, the least cost penalty to the price of electricity. This process employs entrained flow gasifiers (EFGs). Among commercially available EFGs are Shell (Prenflo as well as other name brands), GE (former Texaco) and Mitsubishi gasifiers. To design and operate optimal IGCC plants, there is a need for detailed process simulation, which would ideally be based on computational fluid dynamics coupled with high fidelity physical-chemical submodels for coal conversion. However, comprehensive CFD simulation of gasification are nearly impossible to perform as part of an overall IGCC plant flowsheet model, even for simple gasifier designs let alone one as complex as the Shell process which involves several syngas recirculation and steam production inside the gasifier battery unit. The reduced order model (ROM) developed in [1] has been proposed as an alternative to allow for a reasonably accurate prediction of the gasification process as part of a plant simulation model. In this study, the ROM is modified and implemented in order to predict the performance of the Shell-Prenflo gasifier. Model features, results for a particular reactor size, and sensitivity analysis are presented in this paper.

In section 2, we describe the Shell gasifier and its integration with the rest of the plant. In section 3, the Shell ROM is introduced in detail. In section 4, the geometry and components of the gasifier are presented. Section 5 and 6 describe two important features of this family of gasifiers, the membrane wall and the syngas quench, respectively. Assumptions and methodology are reported in Section 7. In section 8, we present the simulation results while sensitivity analyses are presented in Section 9. Finally, Section 10 is dedicated to the conclusions.

2 Shell-Prenflo Gasification Process

The Shell gasifier is an upflow entrained flow reactor fed with pulverized coal through a number of diametrically opposed burners (4-6) placed in the bottom part of the reactor. The Shell process provides almost separate outlets for the syngas and the ash, with the gas leaving from the top and the larger amount of ash flowing out at the bottom side in the form slag. More than 70% of the ash content in the feed leaves as slag while the remaining stays with the syngas as flyash. The adoption of a dry feed gasifier with high carbon conversion (>99%) leads to higher gasifier efficiency (measured in terms of Cold Gas Efficiency) and higher plant efficiency, when compared to slurry fed gasifiers. Another advantage of the Shell process is the wide variety of coal that can be gasified in this dry-fed system. By using dry gases to pressurize the pulverized coal, there is no limitation on coal composition and the operating conditions. Moreover, the amount of oxygen required for gasification is lower than in slurry fed gasifiers. On the other hand, the gain in cold gas efficiency comes at the cost of higher plant complexity and cost; the higher operating temperature inside the gasifier results in more waste heat and a larger syngas cooler, and requires a water cooled

reactor jacket. Even though the reliability of the dry coal feeding system has been one of the main issues during the initial stages of development, the issue has addressed and it no longer contributes significantly to the total downtime [2].

According to Shell, the gasification pressure is set up to 44 bar; there is a trade-off between the efficiency, which is higher at lower pressures, and the vessel size. Oxygen is produced in an ASU which is partially integrated with the gas turbine (GT) compressor: 50% of the air at the ASU distillation column comes from the GT compressor. Oxygen is fed to the gasifier at 180 °C [3]. Coal is dried before feeding it to the gasifier, limiting its moisture content to 2% by mass, to improve the flow through the lock hoppers and lower the amount of oxidant. The coal carrier is typically nitrogen, produced in the ASU, although it may be replaced by CO_2 for carbon-capture plants. Of the N_2 used for coal feeding, only part flows into the gasifier (around 40-50%), while the remaining is vented during the cyclic operation of the feeding process [4]. Finally a small amount of N_2 is used to regenerate the candle filters for the syngas purification after the convective coolers. The hot syngas exiting the gasifier is quenched to 900°C with cold recycled syngas (at around 200°C). Molten slag entrained by the gas stream solidifies during the quench process while the syngas is cooled to 300°C in the syngas coolers, producing saturated HP and IP steam. The last syngas purification step inside the gasifier train is the wet scrubbing, where the remaining solids and soluble contaminants are removed. Syngas exits the scrubber at about 170°C and, after the regenerative heat exchangers, is sent to a catalytic bed for COS hydrolysis. The latter step is not required in case of pre-combustion CO_2 capture as COS is converted inside the WGS reactor.

Figure 1 shows a detailed representation of the Shell gasification process as described above. Data reported in Table 1 were obtained at the Politecnico di Milano by calibrating the property 0-D code (GS) in order to reproduce the Shell experimental data at the scrubber exit; this simulation is based on chemical equilibrium, adopting the approach-to-equilibrium method. The overall gasification process for a specific coal was reproduced and validated, and it was used to support the kinetic simulation developed in this work, and in assigning the values of oxidant, coal and moderator at the reactor inlet. Different Shell plant configurations based on chemical equilibrium are reported in [5].

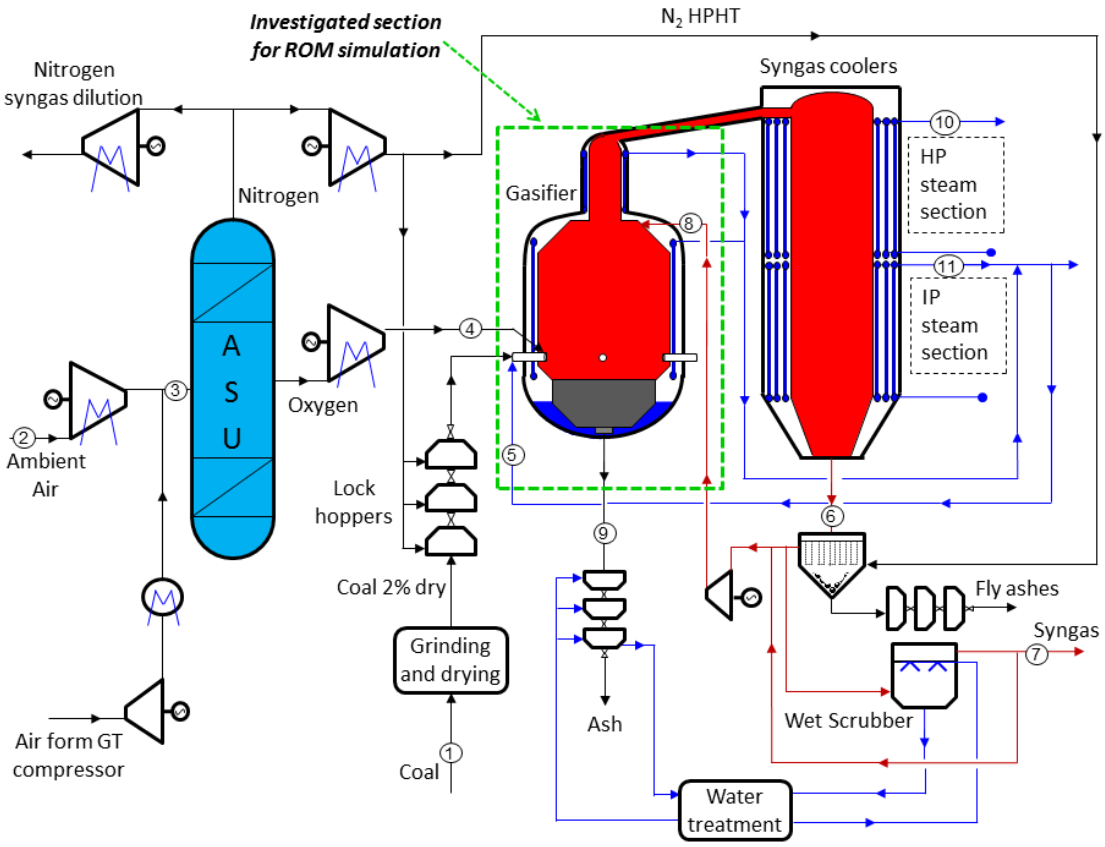

Figure 1: Overview of the Shell gasification process; gases and coal flows are shown in black lines, water in blue and syngas in red; the green dashed line emphasizes the gasifier section investigated in this study and reported with more details in Figure 2.

Table 1: Mass flow, pressure, temperature and composition of the reference Shell gasifier data [6]; data are obtained by calibrating a 0D simulation on the experimental measurements provided by Shell.

Point	G	T	p	Composition, %mol.								
	kg/s	°C	bar	CH_4	CO	CO_2	H_2	H_2O	Ar	N_2	O_2	H_2S
1	35.0	15.0	1.01	Premium Douglas coal as received, see Table 4								
2	60.7	96.0	5.76	-	-	0.03	-	1.03	0.92	77.28	20.74	-
3	121.4	60.7	5.76	-	-	0.03	-	1.03	0.92	77.28	20.74	-
4	29.1	180.0	48.0	-	-	-	-	-	3.09	1.91	95.0	-
5	2.97	300.0	54.0	-	-	-	-	100.0	-	-	-	-
6	115.1	300.0	41.1	0.009	56.66	2.92	26.22	5.09	0.86	8.07	-	.0176
7	76.7	158.5	41.06	0.008	50.55	2.61	23.39	14.47	0.78	8.04	-	0.157
8	49.3	213.8	44.44	0.008	52.22	2.69	24.16	11.66	0.79	8.31	-	0.162
9	5.0	> $T_{melting}$	48.0	Ashes [6]								
10	87.2	339.0	144.00	-	-	-	-	100.00	-	-	-	-
11	7.9	300.0	54.00	-	-	-	-	100.00	-	-	-	-

3 Reduced Order Model

The structure, development and implementation of the Reduced Order Model (ROM) are reported in [1] [7] [8] and [9]. Only the basic concepts of the ROM are briefly described here. In the ROM the gasifier is represented by a Reactor Network Model (RNM). The RNM is based on using idealized chemical reactors (0-D WSR or 1-D PFR) to model different parts of the gasifier. For this reason, the ROM simulation may require some input from CFD. For modeling the current gasifier, the RNM model developed in [7] is chosen, which is based on work in [10] and [11]. The original model was set up for the GE or MHI gasifiers, which are different in several aspects from

the Shell process [12]: i) the wall design (a refractory lining in GE, a membrane wall in Shell and MHI), ii) the flow direction (downward in GE, upward in Shell and MHI), iii) the number of burners (1 in GE, 4/6 in Shell, >4 in MHI), iii) the coal feeding system (wet in GE, dry in Shell and MHI) and iv) the number of stages (one in GE and Shell, two in MHI). The Shell gasifier and the correspondent RNM are shown in Figure 2 while Table 2 reports the geometry data. The Shell gasifier is subdivided into 4 zones:

- IRZ: Internal Recirculation Zone
- JEZ: Jet Expansion Zone
- ERZ: External Recirculation Zone
- DSZ: Downstream Section Zone

The formation of an ERZ downstream of the burner zone is caused by the low value of H/D. The radial dimension of the gasifier allows the stream to expand as it flows downstream with recirculation forming due to the wall impingement. The IRZ zone forms thanks to the high swirl number induced by the injection of coal at a finite angle with the radial direction. One of the main variables affecting the calculation is the diameter and the number of the burners. The cross-sectional area of the JEZ must be equal to the sum of the burners cross-sectional area; this is necessary to avoid unrealistic expansion or compression moving from the IRZ towards the JEZ. Therefore, the Shell ROM is implemented so that, given the geometry and the number of the burners, the JEZ inlet area will automatically have the correct value.

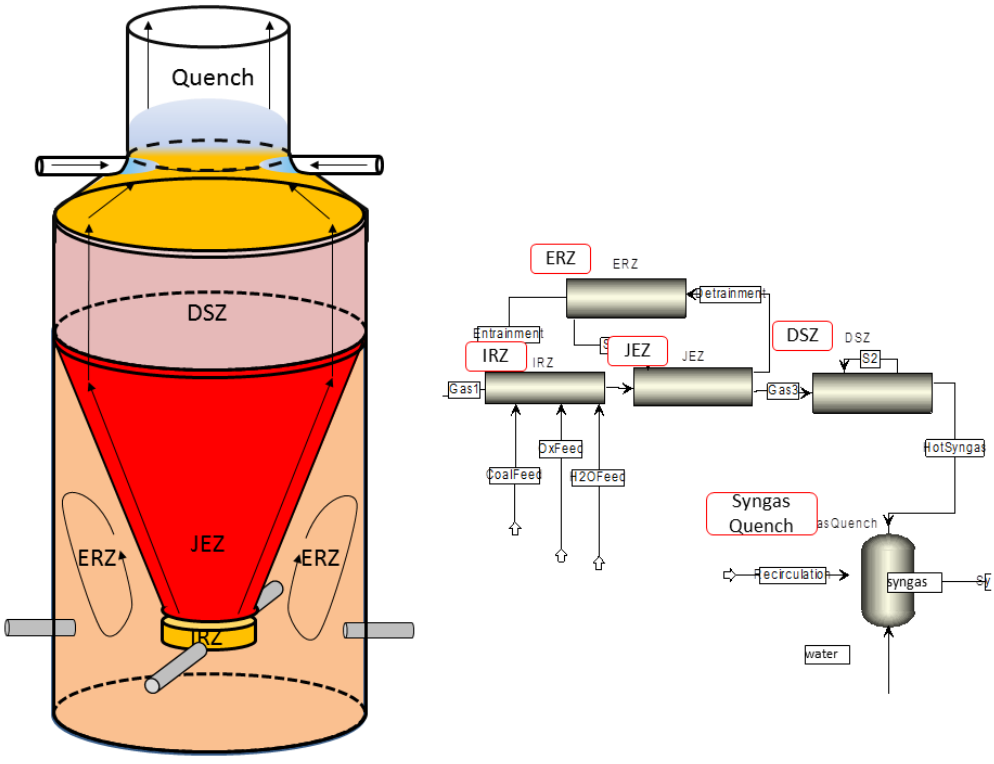

Figure 2: Shell gasifier RNM representation. On the left-hand side the physical macro areas subdivision inside the gasifier; on the right-hand side the equivalent reactor network model in Aspen Custom Modeler.

Table 2: The diameter and length of the gasifier reactor zones

Zone	D inlet [m]	D outlet [m]	Length [m]
IRZ	0.25	0.25	0.20
JEZ	0.50	3.00	7.31
ERZ	n.a	n.a	7.56
DSZ	3.00	3.00	1.44

Figure 3 shows the organization of the ROM model: once the gasifier design is defined (geometry, recirculation ratio after JEZ and expansion angle) the reactors are sized and linked. Each reactor has its own set of conservation equations, 0-D or 1-D if WSR or PFR respectively, which require several submodels to close the system. In the absence of CFD simulations, the parameters for these reactors are chosen based on experience and some modeling. The modular structure of the ROM makes the model flexible and applicable to several types of entrained gasifiers. Once the geometry and the preliminary design are defined, the user can easily switch to different configurations modifying the conservation equations and adjusting the pre-defined parameters [1]. Anyway, a flow field CFD simulation is recommended in order to validate the zone division.

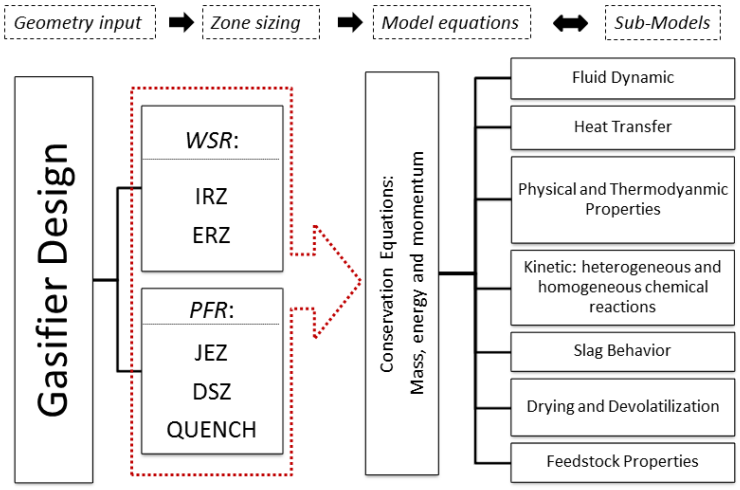

Figure 3: Shell gasifier ROM layout; the gasifier design supplies input to the zone sizing for each idealized reactor. Conservation equations for mass, energy and momentum (both gas and solid) are solved supplemented with several sub-models.

As mentioned above, the recirculation of gases between the JEZ to the ERZ is one of the most important parameter to be assigned. Ideally, it should be provided by CFD simulations [13] [14], which are currently not available for this family of gasifiers. Thus, this value was determined as in [7], using the method of Thring and Newby [15]. The effect of this value on the exit temperature and exit gas molar composition was investigated using sensitivity analysis and reported in Table 3. Results indicate that this sensitivity is very low.

Table 3: The parameters varied in the sensitivity study (temperature and composition at the gasifier reactor outlet) for different values of recirculation ratio. Sensitivity x→y is defined as x/y*(Δy/Δx).

Recirculation ratio	Temperature [°C]		CO dry [%mol]		H_2 dry [%mol]		CO_2 dry [%mol]	
Set value (2.3)	1588.62		63.41		26.40		1.07	
Variation [%]	ΔT [°C]	Sensitivity	CO [%]	Sensitivity	H_2 [%]	Sensitivity	CO_2 [%]	Sensitivity
1.8 (-22.0 %)	-1.4	0.006	+0.015	0.001	+0.022	0.003	-0.023	0.08
2.17 (-6.5 %)	-0.6		+0.004		+0.006		-0.006	
2.47 (+6.5 %)	+0.6		-0.004		-0.005		+0.006	
2.7 (+17.0 %)	+1.3		-0.006		-0.011		+0.011	

4 Geometry and components

The information reported in the next paragraphs were obtained through a comprehensive review of the literature and discussions with Shell for the EBTF project [6]. The gasifier is fed with around 3000 tons/day of coal, a common value for large Shell IGCC plant. The gasifier dimensions for this

size have been inferred and approximated as follows: L = 9m, D = 3m. These values are consistent with recent literature [16] although they have been obtained separately and in different time.

4.1 Burners

The most common burner type is co-annular with coal, a carrier (N_2) and a moderator injected at the center, and oxygen injected from an annular passage [12]. Special attention is given to prevent burner front damage by employing internal cooling, and ensuring the contact of the fresh coal-oxygen stream with the hot syngas inside the reactor to initiate ignition [17]. Two techniques adopted to improve mixing include the use of different injection angles for the oxygen inside the burner before entering the gasifier, and arranging the burner at an angle with respect to the radial direction to create a swirling flow inside the gasifier [18]. Furthermore, the oxygen injector inside the burner can incorporate a swirler to improve mixing between oxygen and coal [12].

Some basic information is required here in order to determine the volume of the IRZ and the boundary conditions with the JEZ. Figure 4 reports the geometry considered, dimensions has been inferred from the Shell patent literature and then adapted to the reactant mass flow considered in this study.

4.2 Membrane Wall

The Shell gasifier is equipped with a water-cooled membrane wall where IP steam is produced inside high-pressure steel tubes all around the reactor jacket. During operation, the primary thermal barrier is provided by the ash layer, composed by a solidified layer attached to the wall and a melted layer which flows towards the bottom of the reactor. A thin layer of castable refractory (generally silicon carbide) is anchored to the tube surface between the steel and the solidified ashes to prevent local damage and corrosion of the membrane wall [19]. As the membrane wall cannot stand large pressure difference, vessel pressurization is maintained by an outer steel vessel which incorporates an air layer between the gasifier outer wall and the membrane wall [12]. On the other hand, the amount of thermal energy removed from the reactor is higher than in the case of a refractory lined gasifier (such as the GE or the MHI). As such, the heat loss calculation is much more complex and critical for the accurate gasifier simulation (see paragraph 5). Heat losses through the reactor walls are in the range of 2-4% of the coal heating value [12].

4.3 Temperature Control

The very short residence time in entrained flow gasifiers (in the range of 1-3 seconds [12]) complicates the control of the reactor operation. The Shell gasifier temperature can be controlled through two different parameters:

- The oxygen/coal ratio, which can provide large variation in the gasification temperature whose average is 1540 °C.
- The gasifier steam production, which can be used to lower the average gasification temperature, but with lower range than the oxygen/coal ratio variation.

In this paper we consider the oxygen to coal ratio to be fixed. The simulation aims to model the process while fixing the incoming gasifier streams as shown in paragraph 2. The results, in terms of the temperature and composition at the outlet, will then be compared with the available data.

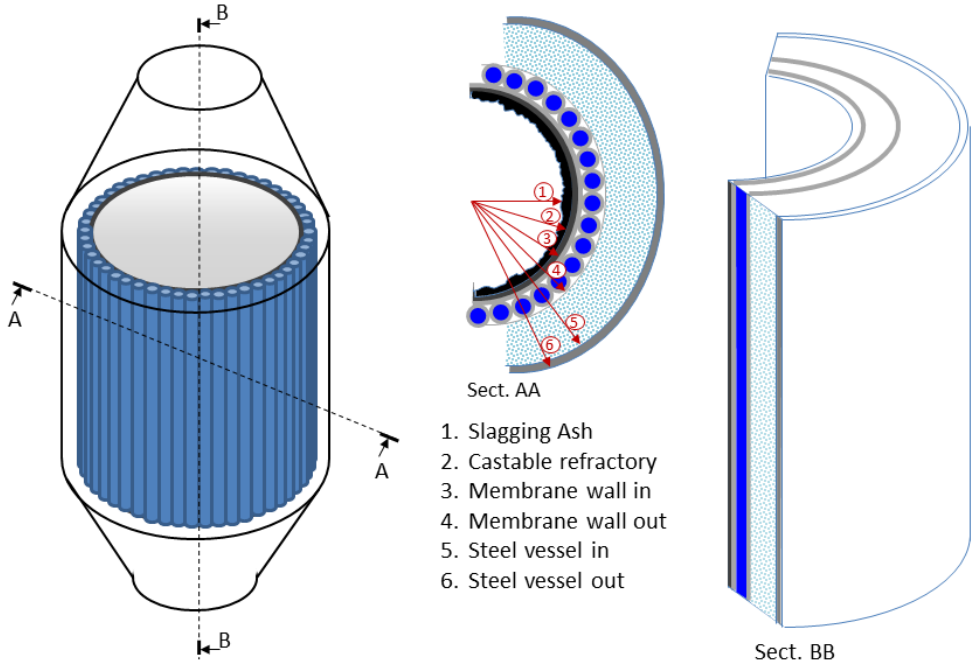

Figure 4: Representation of the Shell gasifier membrane wall; an overall view of the gasifier is shown on the left, horizontal and vertical sections are shown on the right.

4.4 Syngas Quench

The gas quench is carried out at the reactor outlet where the exiting stream temperature is around 1500 – 1600 °C. Most of the syngas cooling is then carried out in the syngas cooler through its membrane wall.

5 Membrane Wall Thermal Model

The membrane composite wall requires heat transfer analysis in the radial and axial directions. Energy balance is written for each wall layer in order to obtain the heat flux and the temperature profile. As shown in Figure 5, the composite wall can be divided into 6 layers:

1. Slag and solid ash layer: the model is based on a single ash layer of variable thickness along the vertical wall, modeling the slag layer built up as molten ash flows from the reactor interior toward the wall. Subdividing the layer into liquid and solid parts [20] would have required many more nodes and would have dramatically increased the cost of the calculations [7]. To analyze the mass and energy balances across a control volume of the slag layer, we consider the following fluxes: (i) the convective flux from gas to wall, (ii) the radiative flux from char particles to the wall, (iii) the mass flow of ash/slag approaching the wall (iv) the mass flow entering and exiting the control volume along the vertical and (v) the conduction flow to the thin castable wall.
2. Silicon carbide (refractory) layer: characterized by high conductivity, this layer receives heat from the attached slag layer releasing it to the membrane wall through conduction.
3. Tube jacket: this is the core of the composite gasifier wall and it is made of a number of vertical water tubes used to cool the wall. The water tubes are in contact with the refractory layer, and the buffer air layer. A steam-water mixture flows inside the tubes. The model must account for the complex heat transfer along the tube. Detailed description of the model is reported in paragraph 5.1.
4. Steam-water mixture: Heat is conducted across the tube walls into the water flowing through the tube, which experiences phase change while flowing upwards. Determining the heat transfer coefficient requires complex calculation, which takes into account the steam-liquid

conditions at each location. Detailed description of the calculation is reported in 5.2. Considering a control volume of steam-water, the energy terms are: (i) the convective heat flow from the tube and (ii) the enthalpy of the incoming/exiting water mixture.

5. Air layer: the tube wall at high temperature transfers heat to the pressurized steel vessel through radiative exchange and to the air layer through natural convection.
6. Steel vessel and ambient air layer: in this final layer, heat is rejected to the ambient air through radiative and convective exchange.

No external insulation has been considered because no reference to external insulation was found. However, it may be required for the safe operation of the plant if the external wall temperature is higher than the safe minimum temperature. This would not make a significant contribution to the gasifier energy balance but it would slightly increase the steam production rate as it lowers the heat released to the ambient.

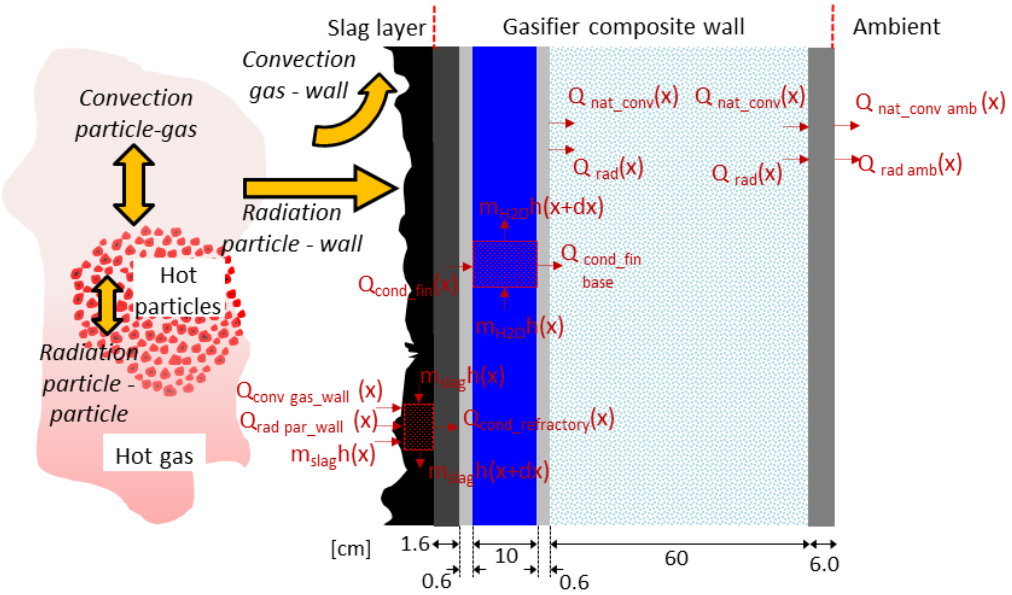

Figure 5: detailed schematics of the gasifier wall with a representation (red) of the heat fluxes considered in the energy conservation equations. Moving from inside to outside, the gasifier wall is composed of: (i) slag layer, (ii) castable refractory, (iii) membrane wall tubes (steel and water), (iv) air layer and (v) steel vessel.

5.1 Equivalent model for the membrane wall

Heat is transferred axially because of the peak temperature near the burners, and radially towards the walls. Nevertheless, because of the temperature distribution and the material heat conductivity, the heat transfer pathways can be simplified: in the radial direction heat flows from the refractory layer to the steel tubes. Indeed, thanks to the high convective heat transfer coefficient inside the tube, almost all the heat is transferred to the water, leaving a small amount to flow to the environment through the outer walls. Thus the tube wall temperature is approximately constant, slightly above the water saturation temperature. This can mathematically be represented using an equivalent fin model as shown in Figure 6. As shown in Figure 6a, half of the tube circumference acts as an extended surface which transfers heat to the water and to the air layer. Considering a pair of half tubes, the extended surface can be modeled as a fin whose thickness is twice the single duct thickness with a prescribed temperature at the fin (Figure 6b). This temperature has to be adjusted in order to satisfy the energy balance across the fin: the conductive heat transfer from the refractory layer must be equal to the convective heat transfer to the water plus the heat transferred to the air layer (both radiative and convective). Conservation of energy allows neglecting the heat transfer to

the air layer, except at the end of the fin. Nevertheless, since the heat transferred to the air is a very small fraction of the total heat transferred to the gasifier wall, the temperature difference along the tube is small making this approximation acceptable.

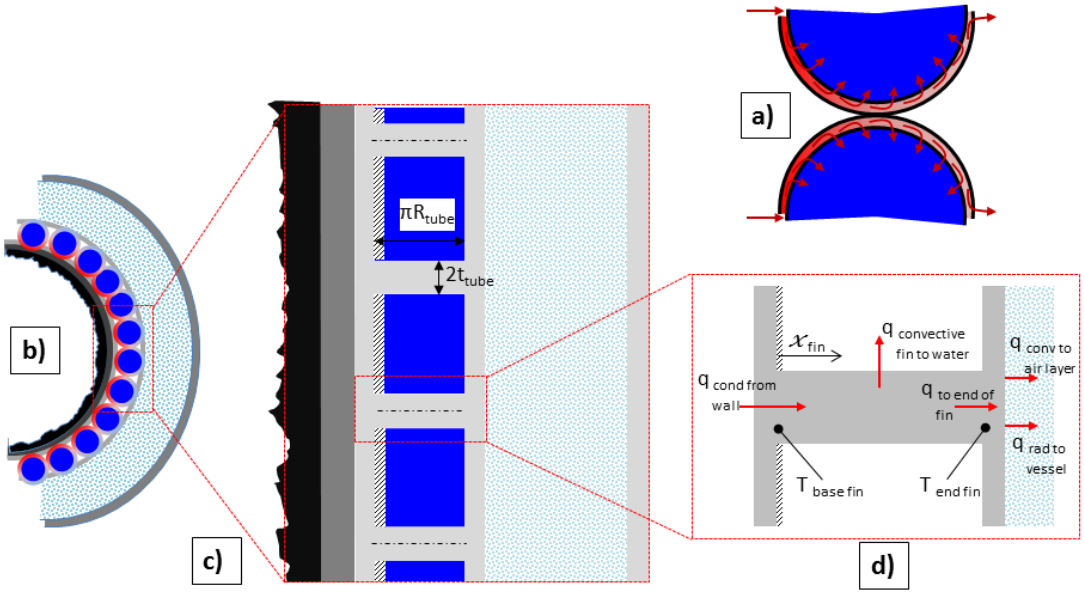

Figure 6: Schematic representation of the equivalent fin model. (a) ideal pathways for the heat along the tube section;(b) horizontal section of the gasifier with emphasis on tube layer; (c) horizontal sketch of the equivalent fin model; (d) detailed representation of one fin with the heat fluxes and main temperatures.

The equivalent fin model is described below. Equation (5-1) and (5-2) show the temperature and heat flux for a uniform cross section fin with prescribed tip temperature; applying the boundary conditions both at the fin base and at the fin end (the temperatures are given once the profile is obtained), the heat flux is obtained and shown in (5-3) and (5-4). The energy conservation equations for the fin base, the coolant flow and the fin tip are written in (5-5), (5-6) and (5-7) respectively.

$$\vartheta(x) = \frac{\vartheta_0 \sinh\big(m(L-x)\big)+\vartheta_L \sinh(mx)}{\sinh(mL)} \tag{5-1}$$

$$q_{fin}(x) = -kA_c\left[\frac{\vartheta_L m}{\sinh(mL)}\cosh(mx) - \frac{\vartheta_0 m}{\sinh(mL)}\cosh\big(m(L-x)\big)\right] \tag{5-2}$$

$$q_{fin}(0) = kA_c\left[\frac{\vartheta_0 m}{\tanh(mL)} - \frac{\vartheta_L m}{\sinh(mL)}\right] \tag{5-3}$$

$$q_{fin}(L) = kA_c\left[\frac{\vartheta_0 m}{\sinh(mL)} - \frac{\vartheta_L m}{\tanh(mL)}\right] \tag{5-4}$$

$$\frac{T_{refractory}-T_{basefin}}{R'_{equivalent}} = q'_{fin}(0) = 2kt\left[\frac{\vartheta_0 m}{\tanh(mL)} - \frac{\vartheta_L m}{\sinh(mL)}\right] \tag{5-5}$$

$$\frac{1}{L}\frac{d\dot{H}}{dx} = q'_{fin}(0) - q'_{fin}(L) = 2kt\left[\frac{\vartheta_0 m}{\tanh(mL)} - \frac{\vartheta_L m}{\sinh(mL)}\right] - 2kt\left[\frac{\vartheta_0 m}{\sinh(mL)} - \frac{\vartheta_L m}{\tanh(mL)}\right] \quad (5\text{-}6)$$

$$q'_{fin}(L) = q'_{rad-air} + q'_{conv-air} \quad (5\text{-}7)$$

The equivalent fin model allows the accurate calculation of the heat transferred to the water using vertical tube boiling correlations for power plant boilers. The flow parameters are calculated for a single tube, results are then extended to all the ducts (i.e. the correspondent equivalent fins).

5.2 Two phase flow heat transfer

Several correlations for two-phase heat transfer are available in literature [21] [22]. For this study, we use a recent correlation proposed by Steiner and Taborek which accounts for the evaporation inside vertical tubes. The local flow boiling heat transfer coefficient is obtained considering convective and nucleate heat transfer obtained from:

$$h_{tp} = \left[\left(h_{nb,0}F_{nb}\right)^3 + \left(h_{Lt}F_{tp}\right)^3\right]^{1/3} \quad (5\text{-}8)$$

The method for calculating the parameters in Equation 5-1 is not discussed here as it is extensively reported in literature [23]. The two-phase flow multiplier F_{tp} is a function of the steam quality, which can be calculated once the heat transfer coefficient has been found; therefore the wall heat problem solution is iterative. The procedure adopted for the temperature profile calculation can be summarized as: the first step lies in the resolution of the energy conservation equations as set by the equivalent fin model; once local water enthalpy has been obtained, all the water properties can be inferred as function of pressure and enthalpy, included the steam quality. Next, h_{tp} is calculated and the temperature profile is obtained.

Particular attention is paid to the conditions reached inside the tube in order to guarantee the system integrity. In particular, steam bubbles must not be allowed to stick to the tube wall as this could lead to local damages. Hence, the steam quality and the inlet velocity must be checked in order to satisfy two conditions: (i) bubble or slug flow inside the tube and (ii) good turbulent wet wall flow; that is, respectively, maximum steam quality of 0.4 and minimum inlet velocity of 0.15 [m/s] [24]. System control is carried out inside the ROM while modifying the global amount of water circulating in the membrane wall.

5.3 Natural convection and radiation inside air layer

Heat inside the air layer is transferred through radiation and natural convection, with the latter less important but still not negligible. The radiative component is calculated assuming radiative heat transfer for long concentric cylinders; emissivity is function of temperature. Due to the high gasifier diameter, plane wall correlation is used to find an approximation of the natural convection term.

6 Syngas Quench and Cooling

The Shell gasification process features several composition and temperature changes not only inside the gasifier but also in the syngas cooler, scrubbing and the COS hydrolysis. As mentioned before, the syngas quench is carried out by mixing hot syngas with cold recirculating syngas. Being at high temperature (syngas leaves the gasifier reactor at 1500-1600°C), cooling and quench are necessary for further reactions. Homogeneous chemical reactions during quench can contribute to hydrogen formation if the water-gas shift rate is sufficient. The WGS reaction inside the quench

depends on the mixing rate: if the mixing rate is fast, the temperature gradient is high with a steep temperature drop at the inlet of the quench zone. In this case, since the uncatalyzed water-gas shift rate is sufficient at least above 1000-1100 °C, hydrogen production is negligible. On the other hand, if mixing is slow along the quench section, the temperature change of the incoming hot gases is slower allowing the WGS to remain reactive. In entrained flow gasifiers, a critical issue which must be addressed is ash sticking on the syngas cooler wall. Fly ash together with other solid particles leaving the gasifier must be cooled rapidly to values below the ash melting temperature, reaching the solid state before approaching the non-slagging wall. That is, mixing has to be vigorous enough to guarantee a high temperature gradient. Although hydrogen production is probably negligible inside the quench zone, kinetic simulation during gas mixing has been implemented in order to make the Shell ROM as flexible as possible.

Under quench operating conditions, the syngas quench zone is modeled as a plug flow reactor with two different choices for the mixing of the fresh and recirculating syngas: (i) perfect mixing at the recirculation inlet, or (ii) progressive mixing along the duct using two discretization zones, ten nodes with user defined mixing ratios. Both cases are not adiabatic but feature the interaction with the wall, which is considered to be a membrane jacket as in the reactor zone.

As carbon conversion is possible only inside the gasifier reactor, we assume that the solid particles are chemically frozen in the quench zone, i.e. no heterogeneous reactions are allowed during quench. The particles are mainly composed by ash and unconverted carbon, which accounts for the carbon left in the particle at the end of gasification. In this zone, particles interact with their environment only via heat and momentum exchange. Being below the melting temperature and having assigned composition, the particle structure is considered fixed along the quench duct.

The primary role of the quench kinetics model is to assess whether the gas mixing is at equilibrium but not to evaluate change in particle composition.

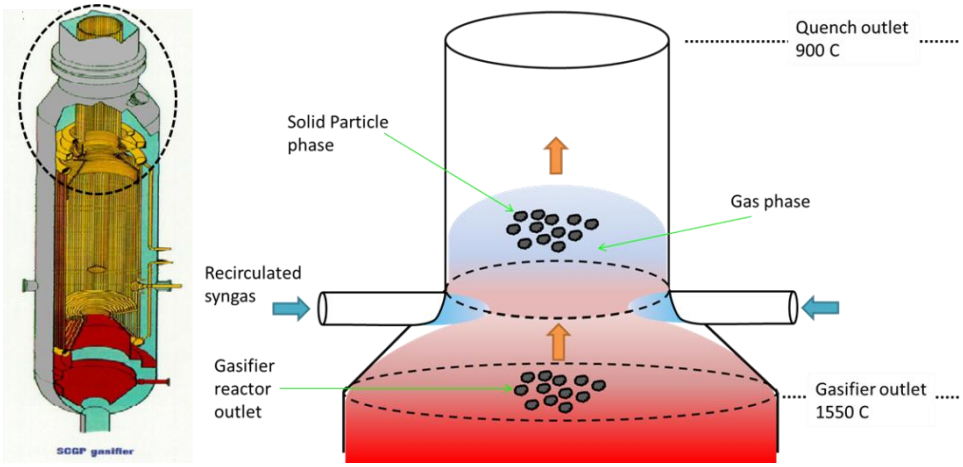

Figure 7: A schematic drawing of the gas quench process; on the left-hand side the quench area of the gasifier, on the right-hand side, a representation of quench process.

7 Assumptions and methodology

The modeling study was carried out using Aspen Custom Modeler®. Aspen Plus® and GS© were adopted in order to model water scrubbing and the overall gasification process, respectively. Coupling these tools, which provide different levels of detail, allows a more comprehensive gasification process simulation. The RNM was developed and solved in Aspen Custom Modeler (ACM), an AspenTech product. ACM is used to create rigorous models of process equipment and

to apply these equipment models to simulate and optimize continuous, batch, and semi-batch processes [25].

GS (Gas-Steam cycles) is a simulation software for energy conversion system developed by GECOS group at Politecnico di Milano. It allows simulating complex systems including chemical reactors, gas treatment units, saturation towers, steam sections with different evaporation levels and many other components for power generation [26].

Other simulation assumptions are reported in Table 4. The membrane wall design has been inferred from available information; Von Mises and Mariotte criteria have been used to check the thickness of the pressurization vessel and the membrane wall tubes respectively. Both thicknesses were sufficient to support the stresses induced by gasification pressure (44 bara) and intermediate steam pressure (54 bara); moreover recent literature [27] reports almost same design values.

Table 4: Simulation assumptions

Ambient conditions	15 °C / 1.013 bar / 60% RH			
Air composition, dry molar fraction (%)	N_2 78.08%, CO_2 0.04%, Ar 0.93%, O_2 20.95%			
Douglas Premium coal characteristics [6]				
Ultimate analysis [%]	C	66.52	O	5.46
	N	1.56	Clorine	0.009
	H	3.78	Moisture	8.0
	S	0.52	Ash	14.15
Proximate analysis [%]	Fixed Carbon 54.9, Volatiles 22.9, Moisture 8.0, Ash 14.15, Total Sulphur 0.52			
Coal LHV, HHV	25.17 MJ/kg, 26.23 MJ/kg			
Oxygen composition	95% O_2, 3.1% Ar, 1.9% N_2			
Oxygen conditions	180 °C, 48 bar			
Moderator steam	300 °C, 54 bar			
Nitrogen for coal feeding (lock hoppers)	80 °C, 88 bar			
Gasifier Geometry				
Height	10 m			
Inner diameter	3 m			
Inner quench diameter	1 m			
Steel vessel thickness	0.06 m			
Gasifier pressure	44 bar			
Membrane Wall				
Tube diameter	0.1 m			
Tube Thickness	0.006 m			
Steel emissivity at 250 °C	0.24			
Steel emissivity at 50 °C	0.22			
Membrane wall internal pressure	54 bar			

8 Results and discussions

The reference simulation was performed using the mass balance reported in Table 1, for a 3000 ton per day of coal. Sensitivity analyses were used to investigate the effects of primary variables.

8.1 Syngas, particles and gasifier wall temperature

Temperature profiles inside the gasifier are shown in Figure 8. The gas and particle temperatures are shown along the centerline whilst the slag temperature is shown at the wall. The gas and particles are in thermal equilibrium for almost all of the gasifier length except in the combustion zone where the volatiles are burnt to supply energy for char gasification. A temperature peak is observed in the combustion zone at the JEZ inlet. The temperature decreases sharply in the

zone where gasification takes place. Following carbon conversion, the temperature changes due to the heat loss to the membrane wall. The temperature decreases a bit steeper in the DSZ than in the last part of the JEZ. Along the JEZ, convective heat transfer to the wall is computed using the gas temperature of the recirculation zone (ERZ) which, because it is modeled as a WSR, is spatially uniform. However this does not affect the radiation term and results in a negligible, although visible, variation.

The computed temperature at the exit is 1588 °C, which is higher than the value assumed for the 0-D simulation reported in paragraph 2 (1550 °C) but still consistent with the temperature range generally provided by Shell (1550-1600 °C) [28] [29] and [30]. The slag temperature refers to the inner value of the slag layer; the corresponding variation along the gasifier is small thanks to the contact with the membrane wall which prevents high temperature peak.

The steam quality and the two-phase heat transfer along the gasifier are shown in Figure 9. The heat transfer coefficient is strongly dependent on the heat flux at the wall; hence the highest value occurs in the combustion zone, decreasing smoothly in the rest of the gasifier. Consequently, steam quality features a steeper increase in the combustion zone where the heat transfer coefficient is higher while it increases in the rest of the gasifier. The outlet steam quality fraction is around 0.25 which is typical of the evaporative section inside large steam generator. This would also fit well with standalone gasifier steam plant.

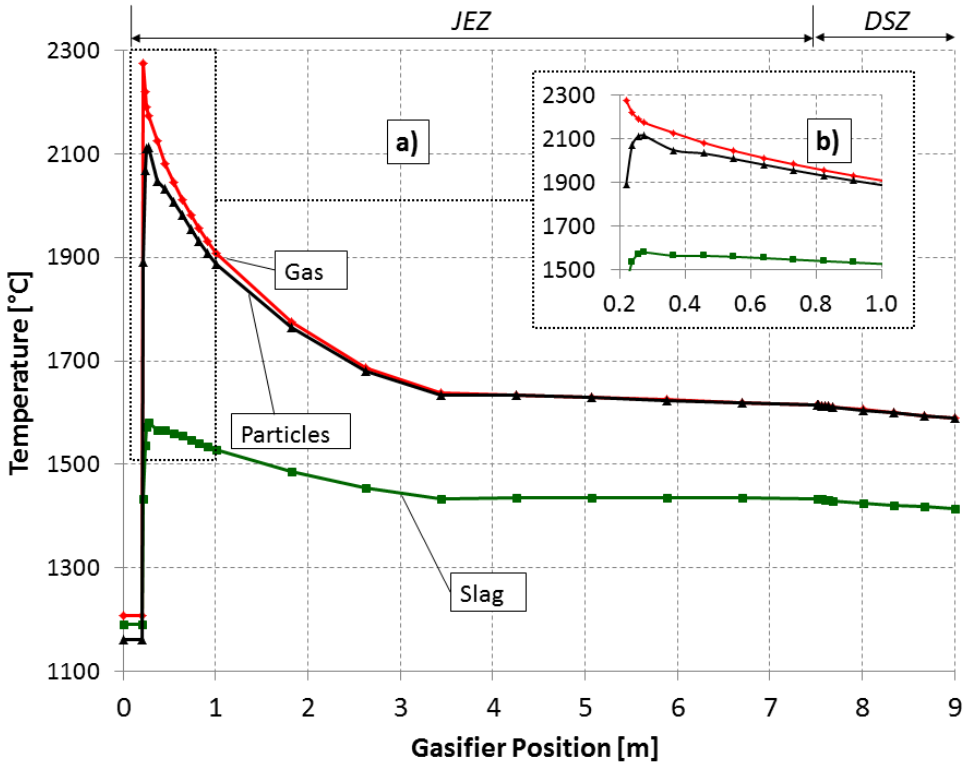

Figure 8: Gas, particle and slag temperature profile inside the gasifier; (a) overall gasifier reactor and (b) details from inlet to 1m height.

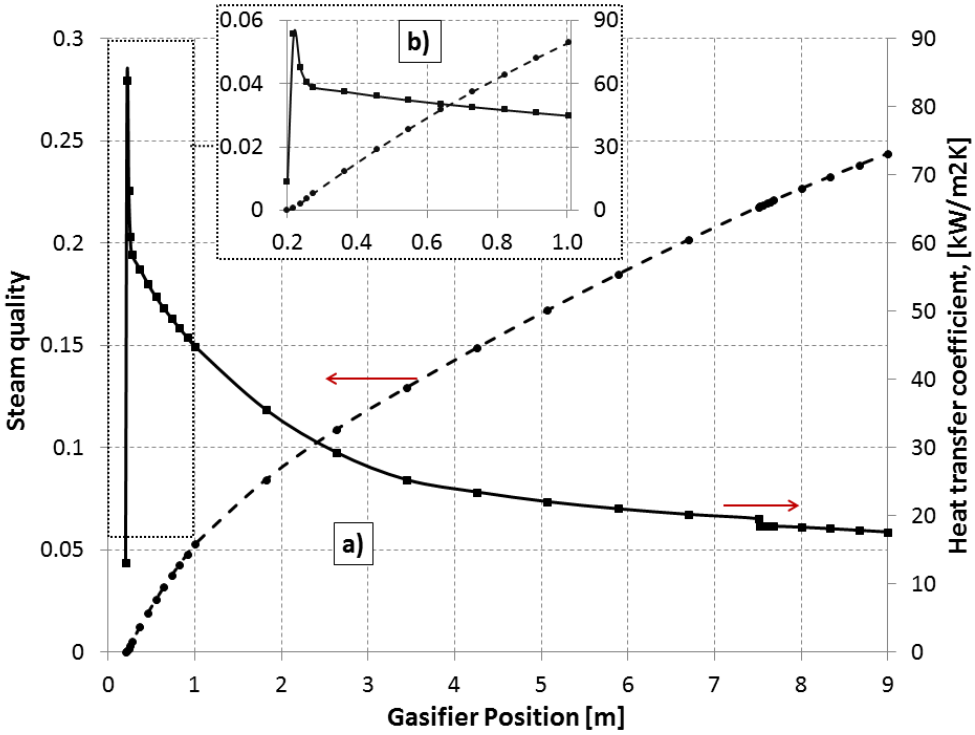

Figure 9: (a) The steam quality and the two phase heat transfer coefficient variation along the gasifier. Steeper steam quality variation is seen in the combustion zone, where the heat transfer coefficient experiences a peak; (b) detail of steam quality and two-phase heat transfer along the first part of the gasifier.

Figure 10 shows the temperature profile along the gasifier wall. The largest temperature gradient is located across the slag layer allowing the membrane walls to stay relatively cool. This is consistent with values obtained in CFD simulations [31] [32]. Moreover, [12] reports that the tubes are almost at the water-steam temperature, within a range of 250-300 °C depending on the evaporation pressure. Nevertheless it must be noted that the ROM underestimates the slag layer thickness (there is no calculation for a liquid-solid interface). The refractory temperature is close to the tube temperature because of the high thermal conductivity of steel compared to the solidified slag. The external vessel temperature is around 50 °C. This is because the air layer thickness guarantees good insulation despite the radiative term.

Figure 11 shows a comprehensive representation of the tube temperature along the entire gasifier length (x-axis), moving from the inside to the outside (y-axis). The temperature variation is reduced by the high two-phase heat transfer value; therefore the tube temperature is within the range of 280-260 °C. Accordingly, the peak temperature is located in the combustion zone.

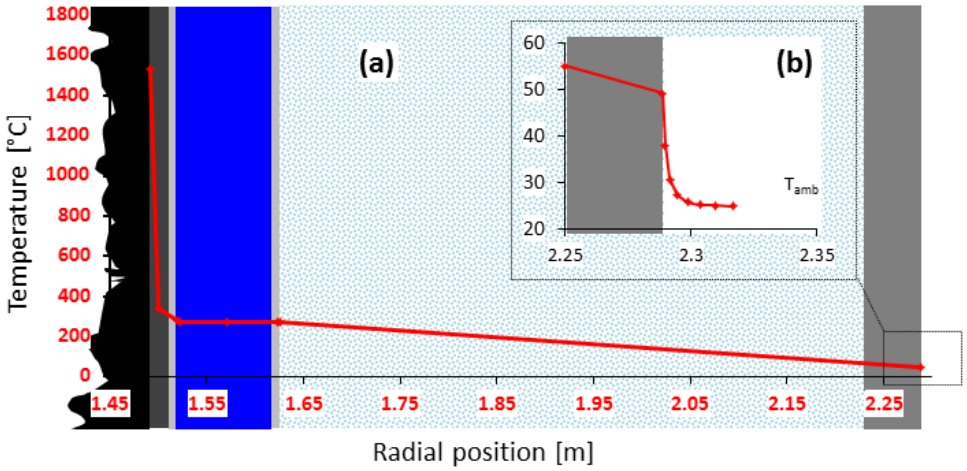

Figure 10: (a) The temperature profile along the gasifier composite wall; slag, refractory, tube, evaporating water, air layer and steel vessel. Values refer to the middle position of the overall height; (b) detail of the temperature profile at the steel vessel - ambient interface.

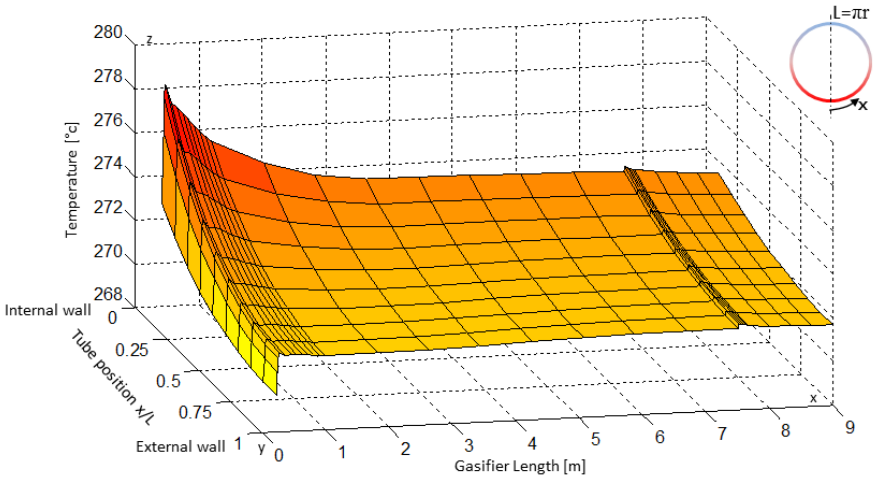

Figure 11: The temperature variation along the membrane jacket. On the x axis, the radial position of the tube measured with respect to the overall semi circumference (i.e. 0 corresponds to the inner face while 1 to the external face), on the y axis the gasifier length and on the z axis the temperature distribution. The small step visible around y=8 is due to the sudden change from the JEZ to the DSZ as assumed by the ROM.

8.2 Syngas composition

The gas composition inside the gasifier is shown in Figure 12. At the combustor inlet, inside the IRZ, devolatilization and coal drying take place; all moisture leaves the particles upon heating whilst part of the non-carbon and the carbon species remain in the char after the devolatilization (Merrick model has been adopted here [1]). The products of devolatilization are: char, CH_4, C_2H_6, CO, CO_2, tar, H_2, H_2O, NH_3 and H_2S. As the mixture enters the JRZ, O_2 is almost instantaneously consumed; H_2O and CO_2 are formed as a result of the combustion of H_2 and char with O_2. As the particle-gas mixture leaves the combustion zone, char gasification takes place; H_2O and CO_2 decrease due to hydro-gasification, the water-gas shift and Boudouard reaction. Hydrogen increases thanks to the WGS. As shown in Figure 13a, the most important heterogeneous reaction is the hydro-gasification which has the highest rate, the Boudouard gasification reaction, and partial combustion are noticeable although the reaction rates are respectively one or two order of magnitude lower than the water gasification. According to the simulation results shown in Figure 13b, almost complete carbon conversion is already reached few meters after the inlet; this seems to be a common feature of most commercial entrained flow gasifier, especially GE and Shell, and it is

consistent with several CFD simulations [33]. This result can be explained considering that the initial gasifier designs have probably been conservative; it would also be consistent with the recent operator tendency to increase the coal feedrate to the same gasifier (till 4500 tons/day for a Shell gasifier). Finally, it must be underlined that the power-law kinetic tends to predict higher conversion rate.

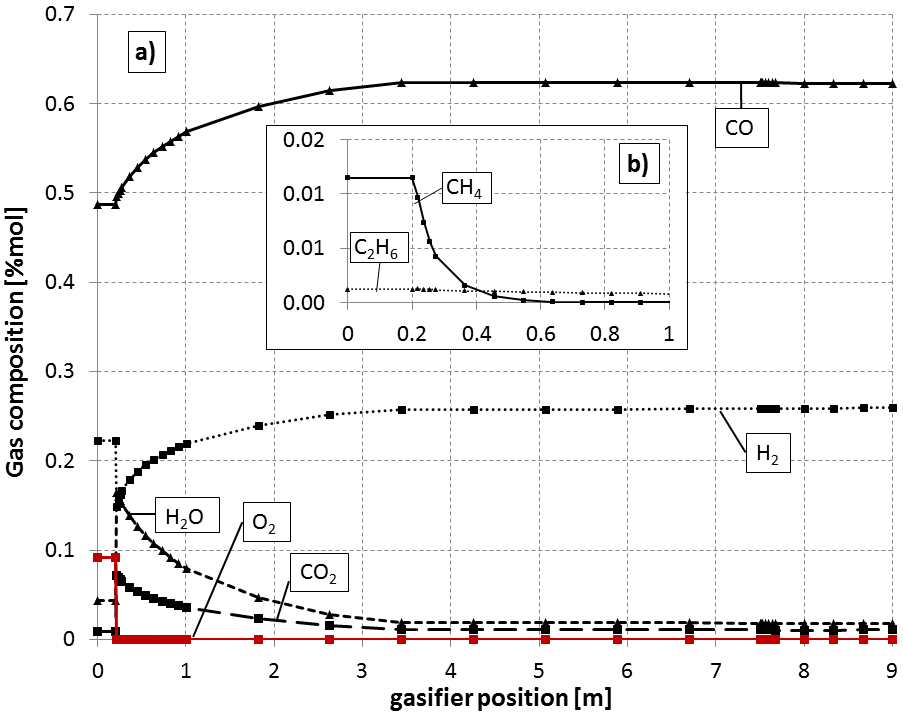

Figure 12: Gas species molar composition along the gasifier; (a) CO, H_2, O_2, H_2O, CO_2, (b) Zooming at gasifier inlet for CH_4 and C_2H_6.

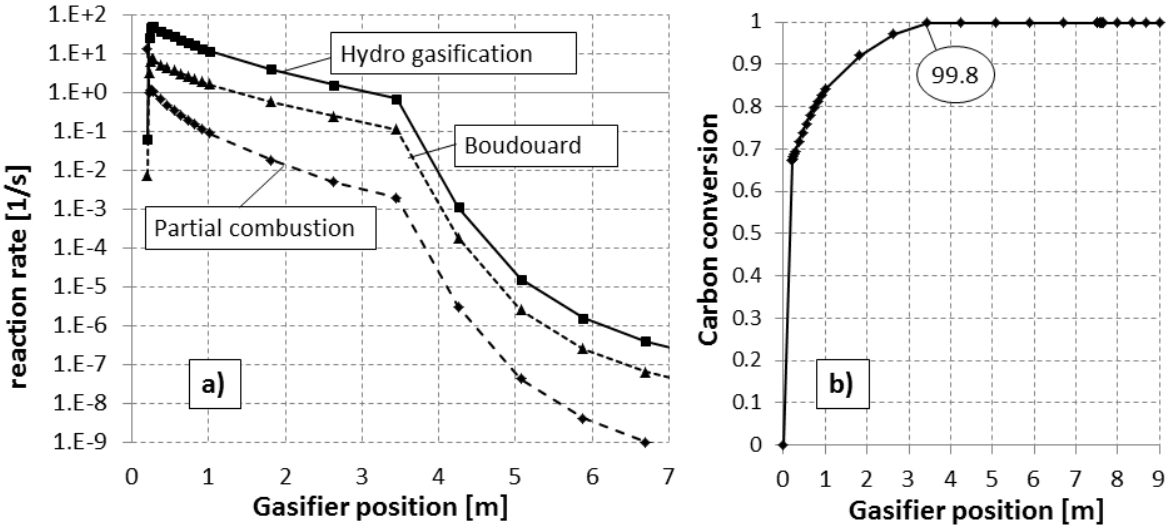

Figure 13: (a) The reaction rate profile along the gasifier length for the heterogeneous reactions (steam gasification, Boudouard and partial oxidation); (b) carbon conversion along the gasifier length. The steep drop in the reaction rate in (a) at around 4 m corresponds to approaching the maximum carbon conversion in (b).

The axial velocity and pressure are shown in Figure 14. Once injected in the IRZ, the flow expands in the JEZ reaching the maximum velocity as soon as the expansion starts. Particles peak velocity is lower and is delayed compared to the gas velocity due to the higher solids inertia. Around three

meters after the reactor inlet, the solids and the gas velocity profiles match. The pressure field reflects the velocity profile: after a minimum at the expansion inlet (the region with higher speed) the pressure increases as the gas slows down. To the first approximation, the residence time is function of the gasifier axial velocity profile; minimum values calculated for the higher local velocity are: i) IRZ: 0.003 [s], ii) JEZ: 0.616 [s] and iii) DSZ: 0.952 [s]. Because the gasifier is operating at steady state, the recirculation zone does not affect the total residence time. Hence, considering the IRZ, the JRZ and the ERZ the total residence time is about 1.6 [s], a value consistent with the residence time for entrained flow gasifiers reported in [12] (1-5 [s]).

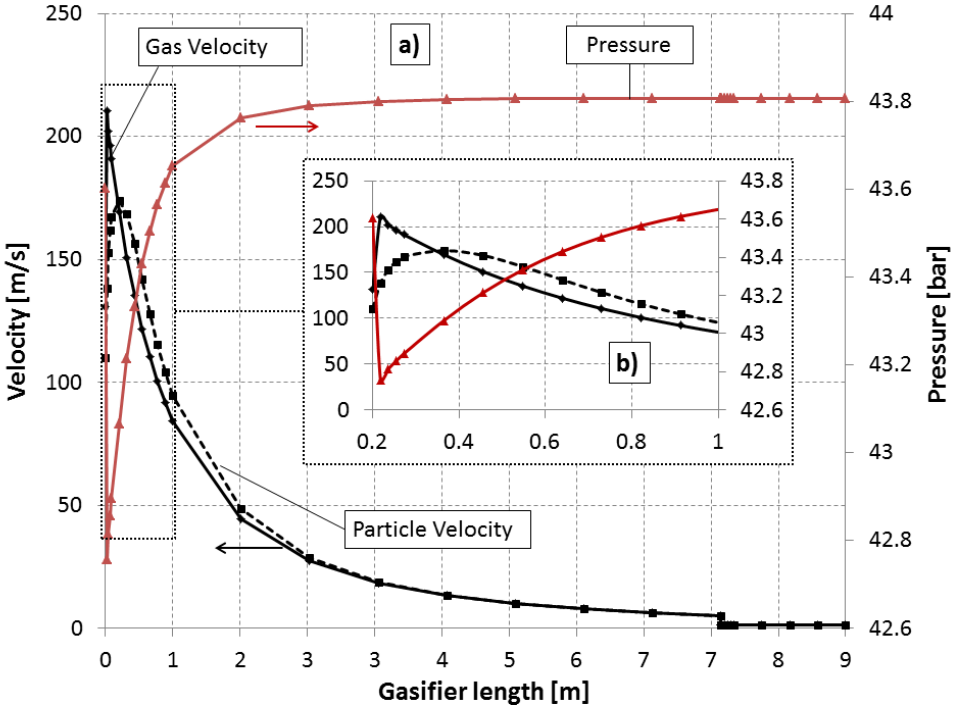

Figure 14: The gas velocity, particle velocity and pressure along the gasifier. The pressure and velocity are linked in the momentum equation. The steep decrease of velocity along the boundary from JEZ to DSZ is are caused by the drop in the mass flow arte due to recirculation.

8.3 Overall gasification temperature and composition

The overall gasification process can be represented by three different zones, placed at the outlet of: i) the gasifier reactor, ii) the quench exit and iii) the scrubber exit. The ROM provides detailed information for both the gasifier reactor and the quench, whilst scrubber process has been simulated in Aspen Plus. Table 5 shows the temperature, pressure, mass flow and molar composition for the gas phase at the outlet of abovementioned sections. The change in molar composition along the quench is mainly due to the mixing with the recirculated syngas partially after the convective coolers and partially after the scrubber. The scrubber process can be represented as saturation and gas purification which does not affect the chemical composition but only the water content. One of the main objectives of this study was to develop a kinetic simulation which could reproduce the gasification process without requiring calibration against supplied composition data (for example adjusting the degree of reaction or the approach to the equilibrium). Table 5 reports a comparison between the ROM results, the equilibrium results for the same flow and the Shell data (available only at the scrubber exit). The equilibrium case does not consider methane formation throughout the gasifier and reflects only gas phase equilibrium, i.e. an equivalent gas composition for incoming coal is adopted which satisfy atomic balance and LHV-HHV values.

Equilibrium simulation produces results close to the ROM as far as the gasifier reactor outlet is concerned; this, as shown in Figure 12 and Figure 13, is due to the fast complete char conversion in the gasifier. It must be emphasized that the equilibrium model is limited to the gas phase and does not describe the solid particle behavior. Larger differences arise when quench is considered; equilibrium calculations are affected by the higher conversion of CO due to water-gas shift. Outlet quench temperature is higher thanks to the heat released by the exothermic reaction. The scrubber process is not affected by the chemical reactions; hence the differences are only due to the incoming composition (the temperature and pressure are the same after the syngas coolers). According to the results shown in Figure 15, where it is also compared with the data provided by Shell, the final dried gas composition calculated using equilibrium is influenced by the overprediction of carbon dioxide and hydrogen. On the other hand the ROM model predicts lower H_2 and CO_2 content, i.e. lower WGS reaction rate. The cold gas efficiency is few percent points above 80%, which is in good agreement with typical Shell values, here available only after the scrubber. The ROM predicts 82.5%, very close to reference 82.8%. Equilibrium case CGE is lower, 82.0%, due to higher CO conversion. From an overall process point of view, the gasification itself accounts for most of the efficiency loss while only 0.7 percent points are lost in the quench and the scrubbing process (0.9 for the equilibrium case). The cold gas efficiency at the quench exit is not meaningful due to the gas recirculation. The results predicted by the equilibrium model are meaningful as long as CH_4 is excluded from reactions, most of all during the quench, otherwise around 1% of methane would be present at the scrubber outlet.

Table 5: Temperature, pressure, mass flow, composition and cold gas efficiency for the gas phase at the most relevant points of the gasification process. Values are reported using the ROM developed in this paper and for an equilibrium model with the same boundary conditions. CGE for Shell data are calculated using the syngas composition reported in this table [34].

	T [°C]	p [bar]	G [kg/s]	Chemical species molar concentration [%mol]								CGE [%]
				CO	H_2	CO_2	H_2O	CH_4	H_2S	N_2	Ar	
Kinetic ROM model												
Gasifier exit	1588.0	43.8	65.9	62.28	25.93	1.05	1.78	--	0.17	7.87	0.91	83.2
Quench exit	932.0	43.8	115.1	58.20	24.32	0.99	7.50	--	0.15	7.97	0.87	--
Scrubber exit	160.6	41.1	76.7	51.90	21.72	0.84	16.70	--	0.13	7.94	0.77	82.5
Equilibrium model												
Gasifier exit	1536.6	43.8	65.9	62.09	25.91	1.16	1.87	--	0.19	7.88	0.91	82.9
Quench exit	1001.2	43.8	115.1	55.32	27.66	4.32	3.59	--	0.18	8.07	0.86	--
Scrubber exit	154.0	41.1	76.7	48.98	24.53	3.65	13.96	--	0.15	7.98	0.76	82.0
Shell data												
Scrubber exit	165.0	41.0	--	48.74	22.37	2.34	17.97	0.02	0.13	7.37	0.95	82.8

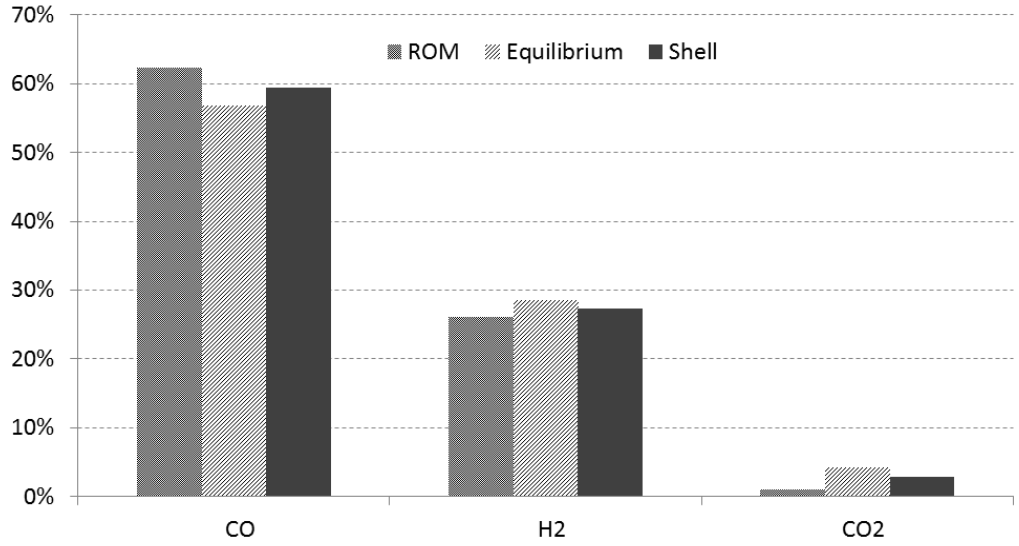

Figure 15: The dry molar gas concentration obtained using the kinetic ROM model, the equilibrium model and Shell data at the scrubber exit.

Results reported in Figure 15 are limited to the gas phase because of equilibrium. Shell data fall in the range between ROM and equilibrium and this is probably related to the WGS activity during the quench. This is directly related to the mixing process in the first part of the quench and it would require a more detailed fluid dynamic simulation (CFD). Indeed, the actual mixing process features several non-ideal effects which affect the temperature gradient inside the flow and, therefore, the WGS activity in this section: a vigorous mixing implies a large temperature change and a lower CO conversion along the quench. This is consistent with the results shown in Figure 15: the perfect mixing model adopted in this ROM simulation lowers the WGS activity as compared to the actual non-perfect mixing case. Regarding the equilibrium results, they are close to Shell data. However the simulation process does not provide as much information as the ROM and requires specific calibration using given operator data.

Figure 16 reports the gas and solid particles temperature profiles for: gasifier reactor, quench, convective coolers and scrubbing. The slag temperature is reported only for the gasifier reactor. If perfect mixing is assumed at the quench inlet, the temperature falls immediately down to around 1000 °C; in the following quench section, cooling is due to the membrane wall heat loss. Syngas is cooled in the convective heat exchangers from 930 °C to 300 °C. Finally, the gas supplies heat for water evaporation in the scrubbing process leaving it at around 160 °C.

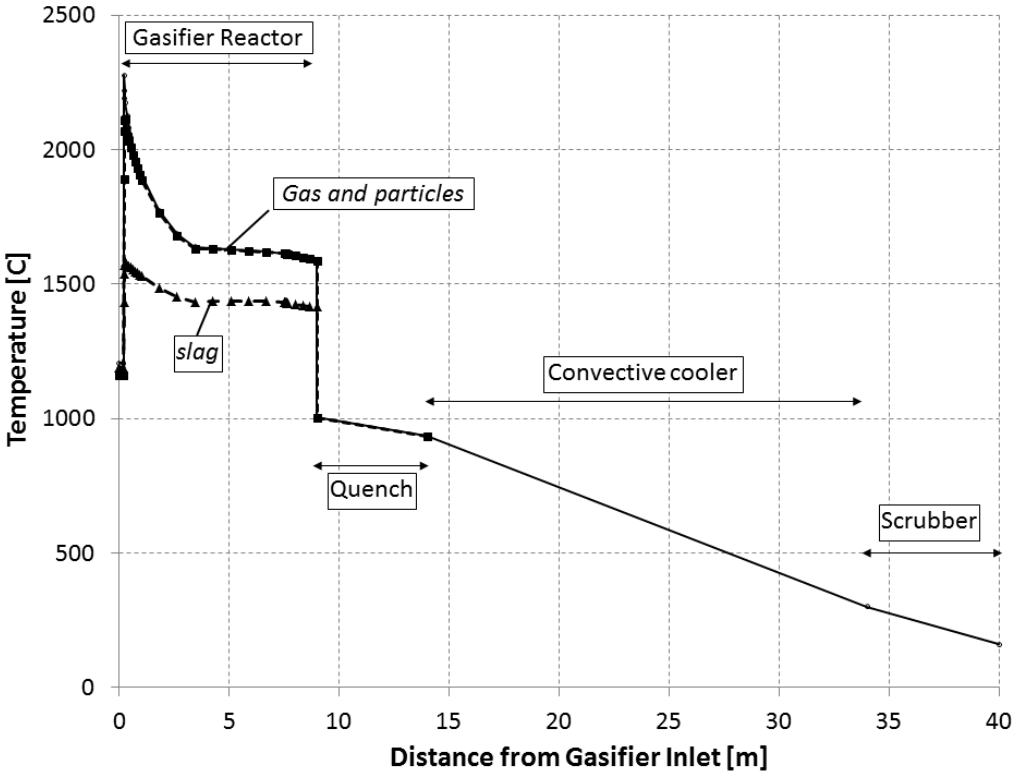

Figure 16: The overall temperature profile for the gasification process; the temperature is reported as function of the distance from the gasifier inlet, syngas cooler and scrubber length are set as 20 and 5 [m] respectively.

9 Sensitivity Analysis

9.1 Oxygen-to-coal ratio

The oxygen needed for the gasification process is one of the most important parameters: it strongly affects the conditions inside the gasifier and contributes to the efficiency penalty. The ROM kinetic model allows predicting accurately the chemical response of the process when boundary conditions change. When the oxygen-to-coal ratio is lowered, the 99.8 carbon conversion is achieved few meters downstream of the location predicted for the base case. In the meantime, the temperature is lower all along the reactor: while oxygen is still abundant at the combustor inlet, the peak temperature is lower but without changing dramatically. On the other hand, within the gasification zone, the lack of thermal energy due to oxygen depletion is balanced by the reactants sensible energy; this results in a lower outlet temperature. As shown in Table 6, gas composition at the gasifier exit reflects the described mechanism: CO molar composition slightly increases as less carbon is burned. Moreover, more carbon is gasified by steam and the water percent sharply decreases. CO_2 content is lower because less is produced in the combustion zone; the Boudouard reaction also consumes more CO_2 along the reactor. This behavior is confirmed by the extrinsic reaction rate in the combustion zone: switching from O/Coal = 0.83 to O/Coal = 0.78, the carbon combustion reaction rate decreases from 13 to 5.8 [s^{-1}] respectively. On the other hand the steam gasification and Boudouard reaction rates are significant for a longer part of the reactor: for O/Coal = 0.78 reactions rates approach zero at around 7.5 meters from the inlet instead of 3.5 (base case). Results obtained in this analysis and reported in Figure 17, show high sensitivity towards oxygen availability: by lowering the oxygen flow by about 6% the reactor length required to reach near complete carbon conversion almost doubles while the exit temperature decreases by about 9%. This is quite different from the results reported in [16] where oxygen sensitivity seems too low.

Table 6: molar concentrations at gasifier reactor outlet for CO, H_2, CO_2 and H_2O; CO

O_2/coal	CO	H_2	CO_2	H_2O
	Molar composition [%]			
0.83	62.28	25.93	1.05	1.78
0.80	62.91	26.91	0.44	0.68
0.78	63.31	27.50	0.02	0.03

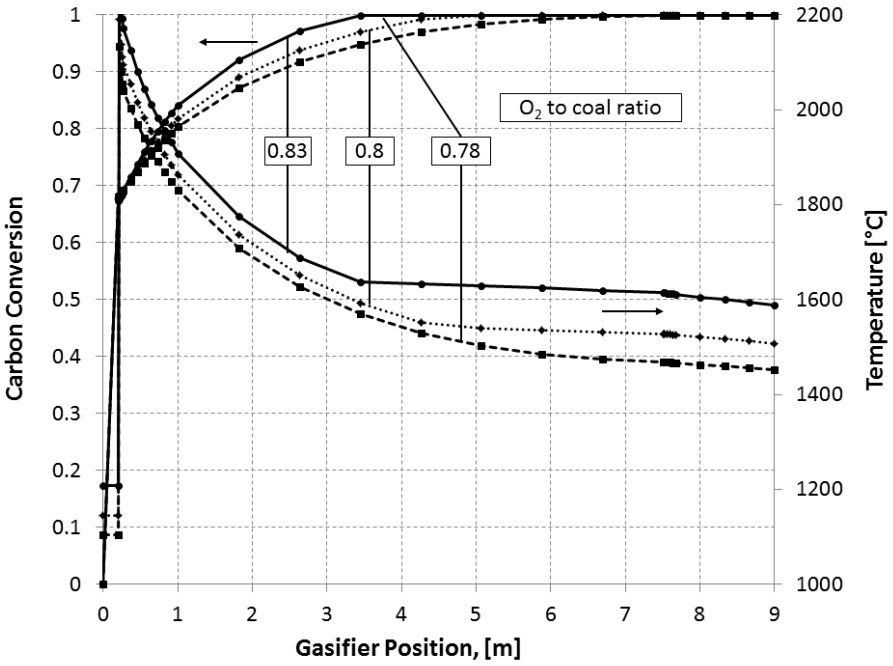

Figure 17: carbon conversion and temperature profile for different oxygen to coal ratios (0.83 = base case, 0.8 and 0.78); influence of oxygen feed on the temperature profile is high: if less O_2 is supplied, carbon conversion slows down and the energy required for gasification lowers the temperature.

9.2 Coal feed Rate

Increasing the coal feed, while fixing the O/Coal, N/Coal ratio, moderator and gasifier geometry, is a reasonable approach to increasing the syngas output at almost constant investment cost. A sensitivity analysis is performed to examine the impact of the coal feed rate. Results are shown in Table 7 and Figure 18. An increase in the coal feed reduces the residence time, the fluid dynamic and transport process, e.g., the gas diffusion towards char particle, but it does not affect the equilibrium chemistry (as O/C and Steam/C are kept fixed). Within the range of values used here, the ROM predicts negligible change in the overall carbon conversion, although as shown in the figure, carbon conversion does slow down. This, while surprising, is not an uncommon observation in operating entrained flow gasifiers, that is, changing the feedrate of coal within a relatively narrow range does not have a significant negative impact on carbon conversion. One reason is that while increasing the feedrate of coal while holding the coal/oxygen ratio constant, the pressure inside the gasifier also increases, speeding up the kinetic rate and overall conversion rate. Changing the flow rate also changes the flow pattern inside the gasifier.

Table 7: residence times for several coal feed rate. For the same gasifier geometry, increasing coal flow rate lowers the residence time in each zone

Coal Input		3500	4000	4500
IRZ	[s]	0.002	0.002	0.001
JEZ	[s]	0.50	0.43	0.38
DSZ	[s]	0.76	0.66	0.58

Tot	[s]	1.26	1.09	0.96

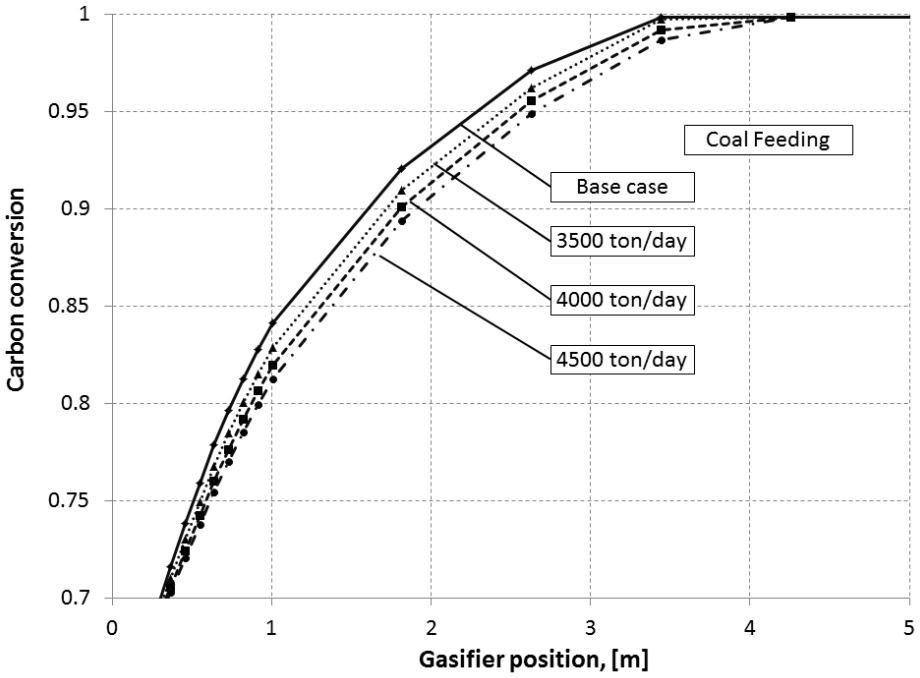

Figure 18: carbon conversion profiles for several coal feed rates. Carbon conversion curves are smoother for higher feedrates, reaching 99.8% at longer distance from the reactor inlet.

9.3 CO_2 feed

Dry feed endows the Shell gasifier with flexibility regarding the coal type. Nitrogen is usually used to charge the lockhoppers. In some applications such as CCS or Fischer-Tropsch applications (Coal to Liquid), it is important to minimize the diluent content of the syngas in order to increase the CO_2 purity after the separation (i.e. for hydrogen membranes) or to increase the partial pressure of the reactants (for FT liquid). Analysis is performed using CO_2 instead of N_2 to charge the lockhoppers while keeping the steam and oxygen flowrates as constant, as suggested by Shell [3]. CO_2 mass flow is recalculated keeping the volumetric flow for the lockhoppers pressurization the same which causes the mass flow rate to double. Switching feed gas changes the reactor chemistry due to the increase of CO_2 and hence shifting the Boudouard equilibrium. Results are shown in Figure 19 and Table 8. The temperature is lower because of the extra inert in the flow. Moreover the larger contribution of the Boudouard reaction increases the temperature difference as the gasification reactions take place along the reactor. This is confirmed by the increase of CO content at the gasifier exit. Finally, the CO_2 concentration outside the gasifier train rises from 2.3% to 5.75% (the increase between quench exit and scrubber exit is due to the candle filter purge flow). The CGE is higher thanks to the lower combustion reaction rate and the lower mean temperature inside the gasifier, i.e. energy released to the water decreases.

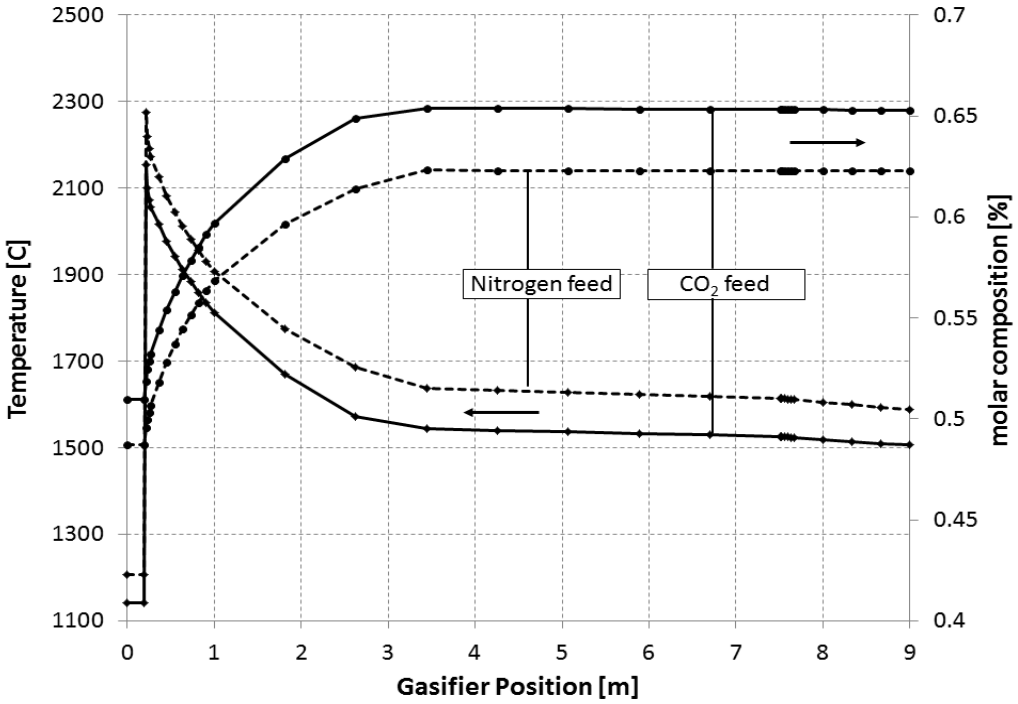

Figure 19: Temperature and CO molar content for gasification with CO_2 and N_2. Higher CO_2 feed raises the mass flow in order to keep the volumetric flow constant at the lock hoppers. The temperature decreases because of the higher feed gas and because of the Boudouard reaction. Likewise, the CO content increases thanks to Boudouard gasification.

Table 8: Temperature, pressure, mass flow, molar content and CGE for gasification with CO_2 feed gas.

	T [°C]	p [bar]	G [kg/s]	Chemical species molar concentration [%mol]								CGE [%]
				CO	H_2	CO_2	H_2O	CH_4	H_2S	N_2	Ar	
Gasifier exit	1505.5	43.8	71.6	65.29	21.21	5.01	5.92	--	0.16	1.33	1.02	83.7
Quench exit	984.0	43.8	111.1	62.21	20.42	5.50	9.43	--	0.16	1.29	0.98	n.a.
Scrubber exit	164.9	41.1	71.6	55.57	18.27	5.75	18.24	--	0.13	1.15	0.88	83.5

10 Conclusions

A reduced order model of the Shell-Prenflo entrained flow gasifier was developed; two well-stirred and three plug flow reactors were used to reproduce each gasifier macro zone. The development of new simulation tools accounting for the wall heat transfer and the quench process allowed reproducing all the features of this gasifier family. The sensitivity analyses with respect to the recirculation level inside the reactor showed that the ROM provides interesting results even without the adoption of a CFD simulation.

The fin-based heat transfer model yields to a peak in the two-phase flow heat transfer coefficient next to the combustion zone where the heat flow is the highest; the calculated steam quality shows the same trend as the heat transfer coefficient. Gas and solid particle outlet temperature is 1588 °C while ashes are around 1400 °C. Temperature variation is strongly non-linear in the first part of the gasifier while it becomes linear when the gasification is almost completed. The tube temperature gradient is limited both along its circumference and axial direction. The ROM predicts quite accurately the syngas conditions at the scrubber outlet; the simulation of the quench mixing resulted to be the main source of difference with the actual process. The equilibrium simulation results are accurate when given gasifier compositions are available for tuning. The CGE predicted by both the ROM and the equilibrium modes are close to

the Shell value; additionally, the ROM can be applied to a variety of coal or with different operating conditions. Sensitivity analyses showed that the ROM is able to accurately predict the chemical behavior such as a change in oxygen feed rate while limits arises when only the fluid dynamic is concerned. Finally, substitution of N_2 with CO_2 as transport gas was investigated highlighting the different gasification regimes for the two cases.

11 Acknowledgements

This study has been carried out thanks to MIT-Politecnico di Milano collaboration funded by Rocca Project framework. The authors wish to acknowledge C. Botero and A. Chapman of RGD Lab at MIT and R.P. Field of MIT Energy Initiative for the support in the Shell ROM developing.

12 References

1. **Monaghan, R.F.D. and Ghoniem, A.F.** A dynamic reduced order model for simulating entrained flow gasfiers. Part I: Model development and description. *Fuel.* s.l. : Elsevier, August 2011. doi: 10.1016/j.fuel.2011.07.015.
2. **Jancker, Steffen.** Delivering performance in Chinese operations. [on-line presentation]. Dresden : s.n., 5 May 2010. http://www.gasification-freiberg.org/desktopdefault.aspx/tabid-16.
3. **Prins, M.** Personal communication. s.l. : Shell.
4. **IEA.** *Potential for Improvement in Gasification Combined Power Generation with CO2 capture.* May 2003. Report Number PH4/19.
5. **Martelli, E, et al.** Shell coal IGCCS with carbon capture: Conventional gas quench vs. innovative configurations. *Applied Energy.* s.l. : Elsevier, 2011. Vol. 88, p. 3978-3989. doi:10.1016/j.apenergy.2011.04.046.
6. **Franco F., Bolland O., Manzolini G., Macchi E., Booth N., Rezvani S., Pfeffer A.** Common Framework Definition document. [Online] 2009. http://caesar.ecn.nl/downloadslinks/.
7. **Monaghan, R.F.D.** Dynamic Reduced Order Modeling of Entrained Flow Gasifier. *PhD thesis.* s.l. : Massachusetts Institute of Technology, February 2010.
8. **Monaghan, R.F.D. and Ghoniem, A.F.** A dynamic reduced order model for simulating entrained flow gasifiers. Part II: Model validation and sensitivity analysis. *Fuel.* s.l. : Elsevier, August 2011. doi:10.1016/j.fuel.2011.08.046.
9. **Monaghan, R.F.D., Kumar, M., Singer, Simcha L, Zhang, C., Ghoniem, A.F.** Reduced Order Modeling of Entrained Flow Solid Fuel Gasification. Lake Buena Vista : s.n. IMECE2009-12985.
10. **Pedersen, L.S., Breithaupt, P., Dam-Johansen, K., Weber, R.** Residence Time Distributions in confined Swirling Flames. s.l. : Taylor & Francis, 1997. Vol. 127. dx.doi.org/10.1080/00102209708935696.
11. **Pedersen, L.S., Glarborg, P., Dam-Johansen, K., Hepburn, P.W., Hesselmann, G.** A Chemical Engineering Model for Predicting NO Emissions and Burnout from Pulverised Coal Flames. s.l. : Taylor & Francis, 1998. Vol. 132. dx.doi.org/10.1080/00102209808952017.
12. **Higman, C. and van der Burgt, M.** *Gasification.* Second Edition. s.l. : Gulf Professional Publishing - Elsevier, 2008. ISBN: 978-0-7506-8528-3.
13. **Kumar, M. and Ghoniem, A.F.** Multphysics simulations of entrained flow gasification. Part I: validating the non-reacting flow solver and the particle turbulent dispersion model. *Energy and Fuels.* s.l. : ACS Publications, 2012. Vol. 26, 1, pp. 451-463. DOI: 10.1021/ef200884j.
14. —. Multiphysics simulations of entrained flow gasification. Part II: constructing and validating the overall model. *Energy and Fuels.* s.l. : ACS publications, 2012. Vol. 26, 1, pp. 464-479. DOI: 10.1021/ef2008858.
15. **Beer J M and Chigier N A.** *Combustion Aerodynamics.* London : Applied Science Publishers, Ltd, 1972. ISBN: 978-0898745450.

16. **Lee, H, Choi, S and Paek, M.** A simple process modelling for a dry-feeding entrained bed coal gasifier. s.l. : Proceedings of the Institution of Mechanichal Engineers, Part A: Journal of Power and Energy, February 2011. Vol. 225, 1, pp. 74-84. DOI: 10.117/2041296710394249.
17. **Klaus Kohnen and Hans Niermann.** *Arrangement for gasifying finely divided particularly solid fuel under high pressure. 4,818,252* [ed.] Krupp Koppers GmbH. United States, March 23, 1987.
18. **Ian Poll.** *Method and Apparatus for the Combustion of Solid Fuel. 4,350,103* [ed.] Shell Oil Company. United States, Spetember 26, 1980.
19. **de Graaf, J.D.** Shell Coal Gasification Technology. *Lecture.* s.l. : Technische Universiteit Eindhoven, 2011.
20. **Yong, S.Z., Gazzino, M. and Ghoniem, A.F.** Modeling the slag layer in solid fuel gasification and combustion - formulation and sensitivity analysis. *Fuel.* s.l. : Elsevier, February 2012. Vol. 92, 1, pp. 162-170. dx.doi.org/10.1016/j.fuel.2011.06.062.
21. **Incropera, et al.** *Fundamentals of Heat and Mass Transfer.* sixth edition. s.l. : Wiley. ISBN: 0-471-45728-0.
22. **Bejan, Adrian and Kraus, Allan D.** *Heat Transfer Handbook.* s.l. : Wiley, 2003. ISBN: 0-471-39015-1.
23. **Thome, John R.** *Engineering Data Book III.* s.l. : Wolverine Tube Inc.
24. **Rayaprolu, Kumar.** *Boilers for Power and Process.* s.l. : CRC Press, Taylor & Francis Group, 2009. ISBN: 978-1-4200-7536-6.
25. **Aspen Custom Modeler.** [Online] AspenTech. http://www.aspentech.com/products/aspen-custom-modeler.aspx.
26. Gecos group. *Energy Department, Politecnico di Milano.* [Online] www.gecos.polimi.it.
27. **Yang, Zhiwei, et al.** Dynamic Model for an Oxygen-Staged Slagging Entrained Flow Gasifier. s.l. : ACS Publications, 2011. 25, pp. 3646-3656. dx.doi.org/10.1021/ef200742s.
28. **Uhde GmbH - ThyssenKrup.** *Press Information No.02.* Dortmund : s.n., 2008.
29. **Volk, Jim.** Shell Coal Gasification: Delivering performance in Chinese operations today, developing technology and deployment solutions for tomorrow. *GTC November 2010.*
30. **Chhoa, Thomas.** Shell Gasification business in action. *GTC October 2005.*
31. **Seggiani, M.** Modelling and simulation of time varying slag flow in a Prenflo entrained-flow gasifier. s.l. : ELSEVIER, November 1998. Vol. 77, 14. dx.doi.org/10.1016/S0016-2361(98)00075-1.
32. **Bockelie, Michale J., et al.** CFD Modeling for Entrained Flow Gasifiers. *Gasification Technologies Conference.* 2002. http://www.reaction-eng.com/downloads/publications.html.
33. **Kumar, M.** Personal Communication. *MIT - Reacting Gas Dynamic Laboratory.*
34. **Shell.** *Information package for DECARBIT: Shell Coal Gasification Process for generic IGCC with carbon capture evaluations.* March 3, 2010.